Illuminating CFTs with the Higher-Point Bootstrap: A Powerful Approach

Valentina Prilepina

November 13, 2025
"Progress of Theoretical Bootstrap", YITP
based on
arXiv:2312.13344 [hep-ph], **arXiv:2507.01223 [hep-ph]**, WIP to appear
with David Poland and Petar Tadić

The Conformal Bootstrap

Conformal bootstrap program seeks to apply symmetries

- conformal, crossing, unitarity, internal

to impose consistency conditions on CFTs

Goal: to map out and solve the space of allowed CFTs

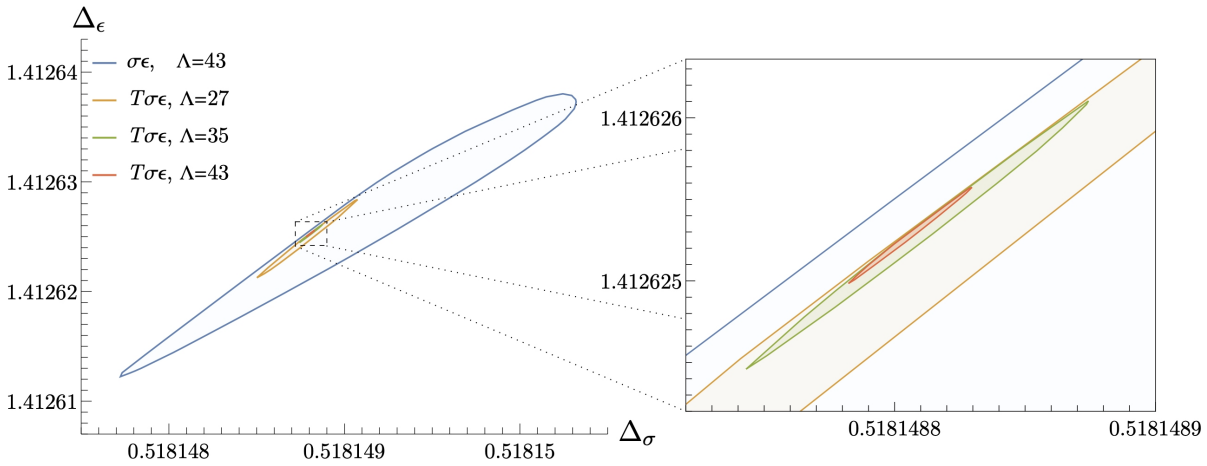

Figure: Allowed regions in $(\Delta_\sigma, \Delta_\epsilon)$-space determined from the $T\sigma\epsilon$ system at $\Lambda = 27, 35, 43$, together with the allowed region determined from the $\sigma\epsilon$ system at $\Lambda = 43$ Kos, Poland, Simmons-Duffin, & Vichi (2016); Chang, Dommes, Erramilli, Homrich, Kravchuk, Liu, Mitchell, Poland, & Simmons-Duffin (2024).

The Ultimate Dream

- Remarkable progress on the numerical and analytic fronts (for reviews, see e.g. Rychkov and Su (2024); Poland, Rychkov and Vichi (2019); Hartman et al. (2022))
- Dream: to classify and solve landscape of CFTs and predict their observables
- To solve a theory $\rightarrow$ to determine its CFT data
  - scaling dimensions of primary operators
  - their OPE coefficients

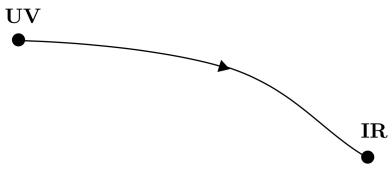

CFTs are lampposts in the landscape of QFTs!

Outline

I. The Higher-Point Bootstrap

- Motivation
- Review of Past Work

II. The Five-Point Bootstrap

- Our Approach
- Five-Point Conformal Blocks
- Approximation Scheme for Truncated Part
- Description of Methods Used
- Results of Numerical Bootstrap
- Comparison to Fuzzy Sphere

III. Comments on Six-Point Snowflake Channel Bootstrap

IV. Conclusions

The Higher-Point Bootstrap: Motivation

Most results extracted by considering 4-point functions!

(for reviews, see e.g. Rychkov and Su (2024); Poland, Rychkov and Vichi (2019); Hartman et al. (2022))

- Explicit expressions/recursion relations for conformal blocks appearing in 4-point functions of scalars in arbitrary d
- Variety of techniques for handling 4-point blocks in arbitrary Lorentz representations

- In principle, can access all CFT data via 4-point bootstrap of external spinning operators, e.g. T
- In practice, this is technically challenging (e.g. Iliesiu et al. (2016, 2018), Dymarsky et al. (2018, 2019), Karateev et al. (2019), Reehorst et al. (2020))

The Higher-Point Bootstrap: Motivation (cont.)

- Recently, most precise results obtained in critical 3d Ising by bootstrapping $(\sigma, \epsilon, T_{\mu\nu})$ (Chang, Dommes, Erramilli, Homrich, Kravchuk, Liu, Mitchell, Poland, and Simmons-Duffin (2024))
- Attractive alternative: to consider **scalar** higher-point functions
- Can access the same CFT data!

Obstruction $\rightarrow$ Higher-point conformal blocks not readily available!

But situation is rapidly changing!

Review of Past Work

Key developments include

- Attempts to bootstrap higher-point correlators both numerically (Poland et al. (2023)) and analytically (Bercini et al. (2020), Antunes et al. (2021), Anous et al. (2021), Kaviraj et al. (2022), Gonçalves et al. (2023), Costa et al. (2023))
- First computation of five-point conformal block for exchanged scalar operators by Rosenhaus (2018)
- Computation of higher-point scalar exchange blocks via holographic methods by Parikh (2019), Hoback and Parikh (2020), Fortin et al. (2022) and by means of dimensional reduction by Hoback and Parikh (2021)

Review of Past Work (cont.)

- Relation between higher-point conformal blocks and solutions of a Lauricella system found by Pal and Ray (2020) and connection to Gaudin models made by Burić et al. (2020, 2021)
- General representations of higher-point scalar exchange blocks developed by Fortin, Ma, Skiba (2019, 2020) using the operator product expansion (OPE) in embedding space
- General representations of 1D and 2D higher-point blocks further developed by Rosenhaus (2018), Fortin et al. (2020, 2023)

Review of Past Work (cont.)

Going beyond scalar exchange in higher dimensions,

- Series expansion for five-point conformal blocks with exchanged spinning operators (and identical external scalars) computed in Gonçalves et al. (2019)
- Recursion relations that reduce a five-point conformal block of arbitrary spin to a finite sum of five-point scalar-exchange blocks derived by Poland and VP (2021)
- Arbitrary five-point conformal blocks computed as a series expansion in radial coordinates by Poland, VP, Tadić (2023)

Five-Point Bootstrap

In the five-point bootstrap, methods cannot use unitarity $\Rightarrow$ no positivity conditions!

- Approach of Poland, VP, Tadić (2023) inspired by truncation techniques of Gliozzi (2013), Gliozzi and Rago (2014)
- Just include contributions in OPE with $\Delta \leq \Delta_{\text{cutoff}}$
- Works, but technically challenging for exchanged spins ≥ 6
- To improve results, need to include more exchanged primary operators

Our Approach

We

- Present an upgraded algorithm for numerical evaluation of five-point conformal blocks in d dimensions similar to Costa et al. (2016)
- Improve accuracy by approximating contributions of $\Delta > \Delta_{\mathrm{cutoff}}$ by counterparts of suitable **disconnected five-point correlator**
- Can compute OPE coefficients involving multiple spinning operators

Five-Point Conformal Blocks

We

- Consider the scalar 5-point function

$$\langle \phi_1(x_1)\phi_2(x_2)\phi_3(x_3)\phi_4(x_4)\phi_5(x_5)\rangle \tag{1}$$

- Decompose it into conformal blocks using OPE in (12) and (45) channels as

$$\sum_{(\mathcal{O}_{\Delta,l},\mathcal{O'}_{\Delta',l'})} \sum_{n_{IJ}=0}^{\min(l,l')} \lambda_{\phi_1\phi_2\mathcal{O}_{\Delta,l}}\lambda_{\phi_4\phi_5\mathcal{O'}_{\Delta',l'}}\lambda^{n_{IJ}}_{\mathcal{O}_{\Delta,l}\phi_3\mathcal{O'}_{\Delta',l'}} \times P(x_i)G^{(n_{IJ})}_{(\Delta,l,\Delta',l')}(u_1', v_1', u_2', v_2', w') \tag{2}$$

- $G^{(n_{IJ})}_{(\Delta,l,\Delta',l')}$ encode contributions of primary STT operators $(\mathcal{O}_{\Delta,l}, \mathcal{O'}_{\Delta',l'})$ in $\phi_1 \times \phi_2$ and $\phi_4 \times \phi_5$

Five-Point Conformal Blocks (cont.)

- Label n_{IJ} enumerates the independent conformally-invariant structures present in $\langle \mathcal{O}_{\Delta,l}\phi_3\mathcal{O}'_{\Delta',l'}\rangle$, with $n_{IJ} = 0, 1, \ldots, \min(l, l')$
- Prefactor $P(x_i)$ given by

$$P(x_i) = \frac{1}{x_{12}^{\Delta_1+\Delta_2} x_{34}^{\Delta_3} x_{45}^{\Delta_4+\Delta_5}} \left(\frac{x_{23}}{x_{13}}\right)^{\Delta_{12}} \left(\frac{x_{24}}{x_{23}}\right)^{\Delta_3} \left(\frac{x_{35}}{x_{34}}\right)^{\Delta_{45}},$$
$$x_{ij} = x_i - x_j \tag{3}$$

- Cross-ratios given by

$$u_1' = \frac{x_{12}^2 x_{34}^2}{x_{13}^2 x_{24}^2}, \quad v_1' = \frac{x_{14}^2 x_{23}^2}{x_{13}^2 x_{24}^2}, \quad u_2' = \frac{x_{23}^2 x_{45}^2}{x_{24}^2 x_{35}^2},$$
$$v_2' = \frac{x_{25}^2 x_{34}^2}{x_{24}^2 x_{35}^2}, \quad w' = \frac{x_{15}^2 x_{23}^2 x_{34}^2}{x_{24}^2 x_{13}^2 x_{35}^2} \tag{4}$$

Computing Five-Point Blocks

In arXiv:2305.08914, we

- Use a suitable ansatz for the 5-point blocks as a series expansion in radial coordinates
  - Unknown coefficients fixed by perturbatively solving two quadratic Casimir differential equations
  - Approach technically challenging for spins ≥ 6

In arXiv:2312.13344, we

- Improve this method to compute blocks for operators of higher spin efficiently

Radial Coordinates

For this, we

- Consider the cross-ratios defined in Burić et al. (2021)

$$
\begin{aligned}
u_1' &= z_1\bar{z}_1\,, \qquad v_1' = (1-z_1)(1-\bar{z}_1)\,,\\
u_2' &= z_2\bar{z}_2\,, \qquad v_2' = (1-z_2)(1-\bar{z}_2)\,,\\
w' &= w(z_1-\bar{z}_1)(z_2-\bar{z}_2) + (1-z_1-z_2)(1-\bar{z}_1-\bar{z}_2)
\end{aligned}
\tag{5}
$$

- Introduce an analog of four-point radial coordinates Costa et al. (2016), Hogervorst and Rychkov (2013)

$$
\begin{aligned}
&z_i = \frac{4\rho_i}{(1+\rho_i)^2}, \quad \rho_i = r_i e^{i\theta_i}\,, \quad \eta_i = \cos\theta_i\,, \qquad i = 1,2\,,\\
&R = \sqrt{r_1 r_2}\,, \quad r = \sqrt{\frac{r_1}{r_2}}\,, \quad \hat{w} = \left(\frac{1}{2} - w\right)\sqrt{(1-\eta_1^2)(1-\eta_2^2)}
\end{aligned}
\tag{6}
$$

The Radial Ansatz

Express the five-point conformal blocks in $(R, r, \eta_1, \eta_2, \hat{w})$ as

$$G^{(n_{IJ})}_{(\Delta,l,\Delta',l')}(R, r, \eta_1, \eta_2, \hat{w}) =$$
$$\sum_{n=0}^{\infty} R^{\Delta+\Delta'+n} \sum_{m} \sum_{j_1,j_2} \sum_{k=0}^{\min(j_1,j_2)} c\left(\frac{n+m}{2}, \frac{n-m}{2}, j_1, j_2, k\right) r^{\Delta-\Delta'+m} \hat{w}^k \eta_1^{j_1-k} \eta_2^{j_2-k}, \tag{7}$$

where

$$\begin{aligned} m &\in [-n, -n+2, \ldots, n-2, n], \\ j_1 &\in \left[\frac{n+m}{2} + l, \frac{n+m}{2} + l - 2, \frac{n+m}{2} + l - 4, \ldots, \mathrm{Mod}\left(\frac{n+m}{2} + l, 2\right)\right], \\ j_2 &\in \left[\frac{n-m}{2} + l', \frac{n-m}{2} + l' - 2, \frac{n-m}{2} + l' - 4, \ldots, \mathrm{Mod}\left(\frac{n-m}{2} + l', 2\right)\right] \end{aligned} \tag{8}$$

The Radial Ansatz (cont.)

Advantages of these coordinates:

- Simplicity of the angular part
- Property that expansion features a single infinite sum over powers of R

Coefficients of ansatz determined by solving two quadratic Casimir equations of the schematic form

$$\left(\sum_i \mathfrak{R}_i(R, r, \eta_1, \eta_2, \hat{w}, \Delta_{12}, \Delta_3, \Delta_{45}, \Delta, \Delta', l, l', d)\partial_i^{p\leqslant 2}\right) G^{(n_{lJ})}_{(\Delta,l,\Delta',l')} = 0 \quad (9)$$

The Radial Ansatz (cont.)

- At zeroth order ($n = m = 0$): $1 + \min(l, l')$ independent functions of η_1, η_2, and $\hat{w}$, $c(0, 0, l, l', k)$ that solve both Casimir equations
- The rest, $c(0, 0, j_1, j_2, k)$ for $j_1 < l$ and $j_2 < l'$, determined in terms of $c(0, 0, l, l', k)$ by solving Casimir equations
- Normalization parameters $c(0, 0, l, l', k)$ depend on choice of 3-point basis
- Use standard box tensor basis Costa et al. (2011) :

$$c(0, 0, l, l', k) = (-1)^{l+l'+k+n_{lJ}} 2^{k+2(\Delta+\Delta')} \binom{n_{lJ}}{k} \tag{10}$$

Speeding up Convergence

- Following Costa et al. (2016), derive recursion relations for c-coefficients
- To evaluate blocks, use a Padé approximant to accelerate the convergence of the series expansion
  - Represent block schematically as

$$G \sim (\#) \sum_{n=0}^{N_{\max}} a_n R^n \tag{11}$$

  - For each (even) value of $N_{\max}$, compute a Padé approximant of G:

$$G_{\text{Padé}} \equiv \left[\frac{N_{\max}}{2} / \frac{N_{\max}}{2} \right]_G (R) \tag{12}$$

Speeding up Convergence (cont.)

- Dependence of $G_{\text{Padé}}$ on $N_{\max}$ typically converges much faster than G
- Same is true for derivatives of G!

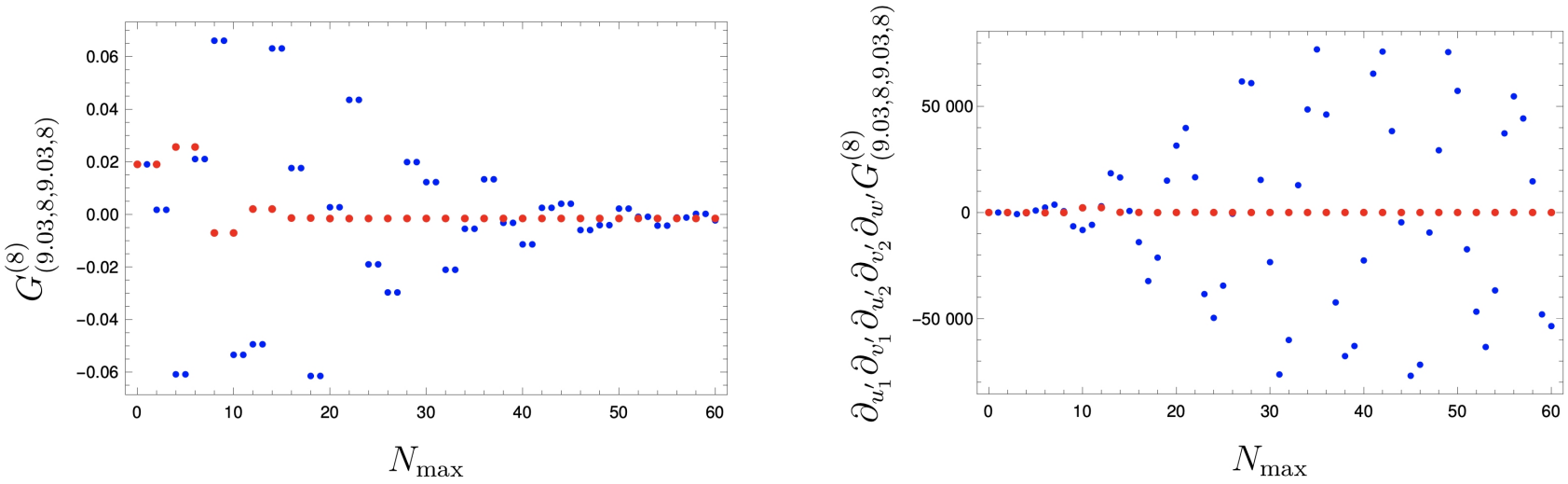

Figure: Five-point conformal block and its derivatives with two exchanged operators of spin 8 with $l = l' = n_{IJ} = 8$, $\Delta_{12} = \Delta_{45} = 0$, $\Delta_3 = 1.413$, $\Delta = \Delta' = 9.03$ evaluated at $R = 2 - \sqrt{3}$, $r = 1$, $\eta_1 = \eta_2 = \hat{w} = 0$

Approximation Scheme for Truncated Part: A Four-Point Example

Consider $\langle\sigma\sigma\sigma\sigma\rangle$ in 3d critical Ising Model and as in Gliozzi (2013), Gliozzi and Rago (2014)

- Truncate the $\sigma \times \sigma$ operator product expansion (OPE) to include only operators with $\Delta \leq \Delta_{\text{cutoff}} \approx 5.022$
- Include operators in $\mathcal{X} = \{\epsilon, \epsilon', T_{\mu\nu}, C_{\mu\nu\rho\sigma}\}$
- ϵ is the leading $\mathbb{Z}_2$-even relevant scalar, ϵ' is a subleading $\mathbb{Z}_2$-even irrelevant scalar, T is the spin-2 stress tensor, and C is the leading spin-4, $\mathbb{Z}_2$-even operator
- Fix conformal dimensions of all exchanged operators Simmons-Duffin (2016)

$$\Delta_\epsilon = 1.412625\,, \quad \Delta_{\epsilon'} = 3.82968\,, \quad \Delta_C = 5.022665 \tag{13}$$

Approximation Scheme for Truncated Part: A Four-Point Example (cont.)

But treat Δ_σ and all OPE coefficients as unknown

$$\mathcal{P}[\mathcal{O}_{\Delta,l}] = \left(\lambda_{\sigma\sigma\mathcal{O}_{\Delta,l}}\right)^2 \tag{14}$$

- Approximate all truncated contributions with the corresponding MFT contributions
- Double-twist operators $[\sigma\sigma]_{n,l}$ of dimension $2\Delta_\sigma^{MFT} + 2n + l$ and spin l in $\mathcal{X}_{MFT} = \{[\sigma,\sigma]_{0,0}, [\sigma,\sigma]_{1,0}, [\sigma,\sigma]_{0,2}, [\sigma,\sigma]_{0,4}\}$

Approximation Scheme for Truncated Part: A Four-Point Example (cont.)

	no MFT	with MFT	Simmons – Duffin (2016)
Δ_σ	0.514(5)	0.5182(4)	0.5181489(10)
$\mathcal{P}[\epsilon]$	1.15(4)	1.106(5)	1.106396(9)
$\mathcal{P}[\epsilon']$	-0.010(8)	0.003(2)	0.002810(6)
$\mathcal{P}[T_{\mu\nu}]$	0.33(5)	0.422(2)	0.425463(1)
$\mathcal{P}[C_{\mu\nu\rho\sigma}]$	0.115(9)	0.0768(5)	0.0763(1)

Table: Numerical data for Δ_σ and unknown OPE coefficients in $\langle\sigma\sigma\sigma\sigma\rangle$ without or with the MFT approximation, compared to best results from Simmons-Duffin (2016)

Compute Δ of operators below Δ_{cutoff} more accurately than in Gliozzi (2013), Gliozzi and Rago (2014) as shown in Li (2023)

Approximation Scheme for Truncated Part: Five-Point Case

We study $\langle \sigma\sigma\epsilon\sigma\sigma \rangle$ in the 3d critical Ising model

- Include all pairs of operators with $\Delta_{\text{cutoff}} = \Delta_C \approx 5.022$: $\{\epsilon, \epsilon', T_{\mu\nu}, C_{\mu\nu\rho\sigma}\}$
- Approximate operators above cutoff by contributions from disconnected five-point correlator

$$\langle \sigma(x_1)\sigma(x_2)\epsilon(x_3)\sigma(x_4)\sigma(x_5)\rangle_d \equiv \langle \sigma(x_1)\sigma(x_2)\rangle\langle \epsilon(x_3)\sigma(x_4)\sigma(x_5)\rangle + (\text{perms.}) \tag{15}$$

- Double-twist operators in $\{[\sigma,\sigma]_{0,0}, [\sigma,\sigma]_{1,0}, [\sigma,\sigma]_{0,2}, [\sigma,\sigma]_{0,4}\}$

Numerical Results: Use of Approximation Scheme

data	without disc.	with disc.
Δ_σ	0.518(2)	0.5181(6)
$\lambda^0_{T\epsilon T}$	0.81(5)	0.96(1)
$\lambda^0_{T\epsilon C}$	0.30(6)	0.48(3)
$\lambda^4_{C\epsilon C}$	-0.3(1)	-0.27(2)
$\lambda^3_{C\epsilon C}$	-2(2)	-0.5(4)
$\lambda^2_{C\epsilon C}$	2(5)	0.1(9)
$\lambda^1_{C\epsilon C}$	-5(11)	-10(1)
$\lambda^0_{C\epsilon C}$	-3(11)	-4(1)
$\lambda_{\epsilon'\epsilon C}$	0(2)	0.9(4)

Table: Numerical data for Δ_σ and unknown OPE coefficients without or with the disconnected correlator approximation

Numerical Results: Use of Approximation Scheme (cont.)

Remarks:

- Results broadly consistent with those of arXiv:2305.08914
- But there is a marked upward shift in central values of $\lambda^0_{T\epsilon T}$ and $\lambda^0_{T\epsilon C}$
- Results for these and the $\lambda^{n_{IJ}}_{C\epsilon C}$ coefficients have smaller errors

Five-Point Crossing Relation

Expand 5-point scalar correlator in (12)(45) OPE channel:

$$\langle \phi_1(x_1)\phi_2(x_2)\phi_3(x_3)\phi_4(x_4)\phi_5(x_5)\rangle = P(x_i)\sum_{\mathcal{O},\mathcal{O}'}\sum_{n_{IJ}=0}^{\min(\ell_{\mathcal{O}},\ell_{\mathcal{O}'})}\lambda_{\phi_1\phi_2\mathcal{O}}\lambda_{\phi_4\phi_5\mathcal{O}'}\lambda^{n_{IJ}}_{\mathcal{O}\phi_3\mathcal{O}'}G^{(n_{IJ})}_{(\mathcal{O},\mathcal{O}')}(u_1',v_1',u_2',v_2',w') \tag{16}$$

Can equivalently expand in (14)(25) OPE channel

OPE associativity $\Rightarrow$ expansions must match!

Five-Point Crossing Relation (cont.)

Crossing relation:

$$\sum_{(\mathcal{O},\mathcal{O}')} \sum_{n_{IJ}=0}^{\min(\ell_{\mathcal{O}},\ell_{\mathcal{O}'})} \lambda^{n_{IJ}}_{\mathcal{O}\phi_3\mathcal{O}'} F^{(n_{IJ})}_{(\mathcal{O},\mathcal{O}')}(u_1', v_1', u_2', v_2', w') = 0, \qquad (17)$$

where

$$\begin{aligned} F^{(n_{IJ})}_{(\mathcal{O},\mathcal{O}')}(u_1', v_1', u_2', v_2', w') = {} & \lambda_{\phi_1\phi_2\mathcal{O}}\lambda_{\phi_4\phi_5\mathcal{O}'}\, v_1'^{\frac{\Delta_1+\Delta_4}{2}}\, v_2'^{\frac{\Delta_2+\Delta_5}{2}}\, G^{(n_{IJ})}_{(\mathcal{O},\mathcal{O}')}(u_1', v_1', u_2', v_2', w') \\ & - \lambda_{\phi_1\phi_4\mathcal{O}}\lambda_{\phi_2\phi_5\mathcal{O}'}\, u_1'^{\frac{\Delta_1+\Delta_2}{2}}\, u_2'^{\frac{\Delta_4+\Delta_5}{2}}\, G^{(n_{IJ})}_{(\mathcal{O},\mathcal{O}')}(v_1', u_1', v_2', u_2', w') \end{aligned} \qquad (18)$$

Five-Point Crossing Relation (cont.)

We

- Study crossing relation for various correlators in 3d Ising
- Truncate the OPE and include small subset of pairs of primaries $\mathcal{S}_{\text{Ising}}^{\langle\phi_1\phi_2\phi_3\phi_4\phi_5\rangle}$
- Approximate truncated contributions by counterparts in

$$\langle\phi_1(x_1)\phi_2(x_2)\phi_3(x_3)\phi_4(x_4)\phi_5(x_5)\rangle_{\mathrm{d}} \equiv \langle\phi_1(x_1)\phi_2(x_2)\rangle\langle\phi_3(x_3)\phi_4(x_4)\phi_5(x_5)\rangle + \mathrm{perm.} \tag{19}$$

Five-Point Crossing Relation (cont.)

In particular: Can write crossing relation as

$$\sum_{(\mathcal{O},\mathcal{O}')\in\mathcal{S}_{\text{Ising}}^{\langle\phi_1\phi_2\phi_3\phi_4\phi_5\rangle}} \sum_{n_{IJ}=0}^{\min(\ell_{\mathcal{O}},\ell_{\mathcal{O}'})} \lambda_{\mathcal{O}\phi_3\mathcal{O}'}^{n_{IJ}} F_{(\mathcal{O},\mathcal{O}')}^{(n_{IJ})}(u_1', v_1', u_2', v_2', w')$$
$$+ \sum_{(\mathcal{O},\mathcal{O}')\notin\mathcal{S}_{\text{Ising}}^{\langle\phi_1\phi_2\phi_3\phi_4\phi_5\rangle}} \sum_{n_{IJ}=0}^{\min(\ell_{\mathcal{O}},\ell_{\mathcal{O}'})} \lambda_{\mathcal{O}\phi_3\mathcal{O}'}^{n_{IJ}} F_{(\mathcal{O},\mathcal{O}')}^{(n_{IJ})}(u_1', v_1', u_2', v_2', w') - 1 = 0 \tag{20}$$

Write similar statement for disconnected correlator and make the approximation:

$$\sum_{(\mathcal{O},\mathcal{O}')\notin\mathcal{S}_{\text{Ising}}^{\langle\phi_1\phi_2\phi_3\phi_4\phi_5\rangle}} \sum_{n_{IJ}=0}^{\min(\ell_{\mathcal{O}},\ell_{\mathcal{O}'})} \lambda_{\mathcal{O}\phi_3\mathcal{O}'}^{n_{IJ}} F_{(\mathcal{O},\mathcal{O}')}^{(n_{IJ})}(u_1', v_1', u_2', v_2', w')$$
$$\approx \sum_{(\mathcal{O},\mathcal{O}')\notin\mathcal{S}_{\text{disc.}}^{\langle\phi_1\phi_2\phi_3\phi_4\phi_5\rangle}} \sum_{n_{IJ}=0}^{\min(\ell_{\mathcal{O}},\ell_{\mathcal{O}'})} \Lambda_{\mathcal{O}\phi_3\mathcal{O}'}^{n_{IJ}} F_{(\mathcal{O},\mathcal{O}')}^{(n_{IJ})}(u_1', v_1', u_2', v_2', w') \tag{21}$$

Five-Point Numerical Bootstrap (cont.)

Obtain approximate crossing relation:

$$\sum_{(\mathcal{O},\mathcal{O}')\in\mathcal{S}_{\text{Ising}}^{\langle\phi_1\phi_2\phi_3\phi_4\phi_5\rangle}} \sum_{n_{IJ}=0}^{\min(\ell_{\mathcal{O}},\ell_{\mathcal{O}'})} \lambda_{\mathcal{O}\phi_3\mathcal{O}'}^{n_{IJ}} F_{(\mathcal{O},\mathcal{O}')}^{(n_{IJ})}(u_1', v_1', u_2', v_2', w') - \sum_{(\mathcal{O},\mathcal{O}')\in\mathcal{S}_{\text{disc.}}^{\langle\phi_1\phi_2\phi_3\phi_4\phi_5\rangle}} \sum_{n_{IJ}=0}^{\min(\ell_{\mathcal{O}},\ell_{\mathcal{O}'})} \Lambda_{\mathcal{O}\phi_3\mathcal{O}'}^{n_{IJ}} F_{(\mathcal{O},\mathcal{O}')}^{(n_{IJ})}(u_1', v_1', u_2', v_2', w') \simeq 0 \tag{22}$$

Five-Point Numerical Bootstrap (cont.)

Fix the conformal data to the values below, extracted from Simmons-Duffin (2016); Chang, Dommes, Erramilli, Homrich, Kravchuk, Liu, Mitchell, Poland, and Simmons-Duffin (2024); Su (unpublished)

Conformal data:

$\mathcal{O}$	$\Delta_{\mathcal{O}}$	$\lambda_{\sigma\sigma\mathcal{O}}$	$\lambda_{\epsilon\epsilon\mathcal{O}}$	$\lambda_{\epsilon'\epsilon'\mathcal{O}}$
ϵ	1.412625	1.0518537	1.532435	2.3955808
ϵ'	3.82968	0.053012	1.536	7.6771
$T_{\mu\nu}$	3	-0.65227552	-1.7782942	-4.8210194
$C_{\mu\nu\rho\sigma}$	5.022665	0.276304	0.99168	–
S_6	7.028488	0.1259328	0.529088	–
X_8	9.031023	0.05896	0.277088	–
X_{10}	11.0324141	0.02801984	0.1433952	–

Table: CFT data for the $\mathbb{Z}_2$-even part of the spectrum in the 3d critical Ising model.

Five-Point Numerical Bootstrap (cont.)

Conformal data:

$\mathcal{O}$	$\Delta_{\mathcal{O}}$	$\lambda_{\sigma\epsilon\mathcal{O}}$
σ	0.5181489	1.0518537
σ'	5.2906	0.057235
Σ_2	4.180305	0.77831882
Σ_3	4.63804	0.39173716
Σ_4	6.112674	0.4308208
Σ_5	6.709778	0.2371098
Σ_6	8.08097	0.2295216
Σ_7	8.747293	0.1313810

Table: CFT data for the $\mathbb{Z}_2$-odd part of the spectrum in the 3d critical Ising model.

Five-Point Numerical Bootstrap (cont.)

Strategy:

- Generate additional constraints by taking derivatives w.r.t. cross-ratios $\mathcal{D}_i$
- Evaluate all constraints at

$$u_1' = v_1' = u_2' = v_2' = 1, \quad w' = \frac{3}{2} \tag{23}$$

- Denote constraints by $e_i(\lambda)$ and define cost function

$$f(r,\lambda) = \left(\frac{1}{\sum_{i=1}^{\mathcal{C}} r_i}\right) \sum_{i=1}^{\mathcal{C}} r_i \left(\frac{e_i(\lambda)}{e_i(0)}\right)^2 \tag{24}$$

- Include constraints in $f(r,\lambda)$ that maximize

$$\mathcal{I} = \frac{\det\left(\left.\frac{\partial^2 f(1,L)}{\partial_{L_i}\partial_{L_j}}\right|_{\min}\right)}{f(1,\lambda)|_{\min}} \tag{25}$$

Five-Point Numerical Bootstrap (cont.)

- Calculate large fixed set of constraints
- For each subset of $\mathcal{C}$ constraints, select constraints with largest $\mathcal{I}$
- Compute OPE coefficients by randomly varying weights r_i
- Expect $\mathcal{C}$ to be large enough to lift flat directions but not too large $\rightarrow$ difficult to satisfy truncated crossing relation
- Optimal balance: Choose values of $\mathcal{C}$ and number of subsets for each $\mathcal{C}$ s.t. results stabilize!
- Finally, merge all results across different $\mathcal{C}$'s and compute total mean and standard deviation

Results of Numerical Bootstrap: $\sigma \times \sigma$ OPE

Consider $\sigma \times \sigma$ OPE and use truncation method to study

- $\langle \sigma\sigma\epsilon\sigma\sigma \rangle$, $\langle \sigma\sigma\epsilon'\sigma\sigma \rangle$
- Include e.g. for $\langle \sigma\sigma\epsilon'\sigma\sigma \rangle$:

$$\mathcal{S}_{\text{Ising}}^{\langle \sigma\sigma\epsilon'\sigma\sigma \rangle} = \{\mathbf{1}, \epsilon, \epsilon', T_{\mu\nu}, C_{\mu\nu\rho\sigma} | \text{ all pairs}\} \tag{26}$$

- Approximate the rest by counterparts from

$$\langle \sigma(x_1)\sigma(x_2)\epsilon'(x_3)\sigma(x_4)\sigma(x_5) \rangle_{\text{d}} = \langle \sigma(x_1)\sigma(x_2) \rangle \langle \epsilon'(x_3)\sigma(x_4)\sigma(x_5) \rangle + \text{perm.} \tag{27}$$

- Subtract contributions from

$$\mathcal{S}_{\text{disc.}}^{\langle \sigma\sigma\epsilon'\sigma\sigma \rangle} = \{[\sigma,\sigma]_{0,0}, [\sigma,\sigma]_{1,0}, [\sigma,\sigma]_{0,2}, [\sigma,\sigma]_{0,4} | \text{ all pairs}, (\mathbf{1}, \epsilon'), (\epsilon', \mathbf{1})\} \tag{28}$$

- Rescale unknown OPE coefficients as in $\lambda^0_{T\epsilon' T} = \Lambda^0_{[\sigma,\sigma]_{0,2}\epsilon'[\sigma,\sigma]_{0,2}} L^0_{T\epsilon' T}$

Results of Numerical Bootstrap: $\sigma \times \sigma$ OPE (cont.)

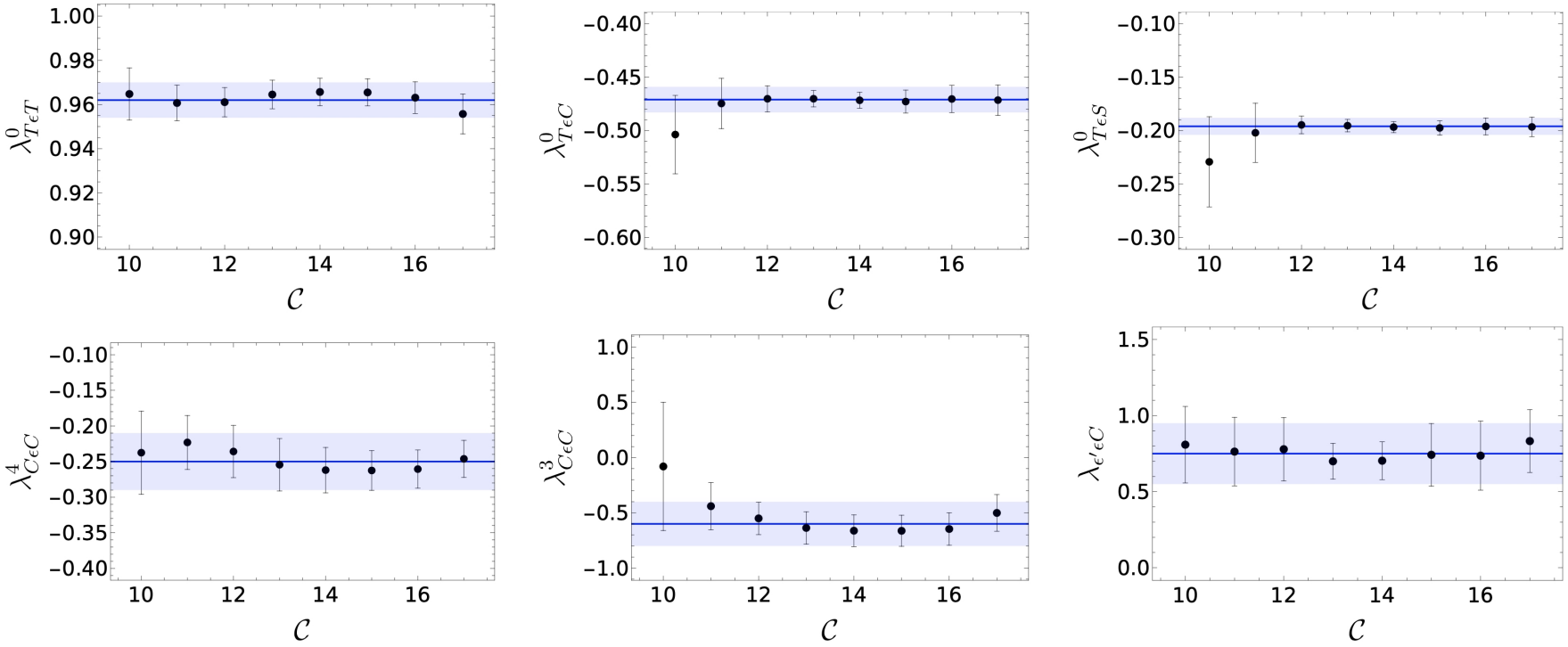

Figure: OPE coefficients computed from $\langle\sigma\sigma\epsilon\sigma\sigma\rangle$ by averaging over the minima of the cost function for the 20 sets of $\mathcal{C}$ constraints with the largest $\mathcal{I}$. Values determined by averaging the results with $12 \leqslant \mathcal{C} \leqslant 17$.

Results of Numerical Bootstrap: $\sigma \times \sigma$ OPE (cont.)

	est. values
$\lambda^0_{T\epsilon T}$	0.962(8)
$\lambda^0_{T\epsilon C}$	-0.471(12)
$\lambda^0_{T\epsilon S}$	-0.196(8)
$\lambda^4_{C\epsilon C}$	-0.25(4)
$\lambda^3_{C\epsilon C}$	-0.6(2)
$\lambda^2_{C\epsilon C}$	1.8(8)
$\lambda^1_{C\epsilon C}$	-8(2)
$\lambda^0_{C\epsilon C}$	-2.9(9)
$\lambda_{\epsilon'\epsilon C}$	0.75(20)

Table: Numerical data for unknown OPE coefficients in the truncated $\langle\sigma\sigma\epsilon\sigma\sigma\rangle$ correlator, obtained from the 20 sets of constraints with the largest $\mathcal{I}$ for $12 \leqslant \mathcal{C} \leqslant 17$.

Results of Numerical Bootstrap: $\sigma \times \sigma$ OPE (cont.)

Remarks:

- $\lambda^0_{T\epsilon T}$ computed using the fuzzy sphere regularization approach: $\lambda^0_{T\epsilon T} \simeq 0.9162(73)$ Hu, He, and Zhu (2023)
- Very precisely computed using mixed four-point bootstrap for $(\sigma, \epsilon, T_{\mu\nu})$: $\lambda^0_{T\epsilon T} = 0.95331513(42)$ Chang, Dommes, Erramilli, Homrich, Kravchuk, Liu, Mitchell, Poland, and Simmons-Duffin (2024)
- Also

$$f_{C\epsilon C} = \lambda^4_{C\epsilon C} - \frac{1}{3}\lambda^3_{C\epsilon C} + \frac{2}{15}\lambda^2_{C\epsilon C} - \frac{2}{35}\lambda^1_{C\epsilon C} + \frac{8}{315}\lambda^0_{C\epsilon C} \quad (29)$$

  estimated to be ~ 0.5 Herviou, Läuchli, Rychkov, and Wilhelm (2025)
- Find $f_{C\epsilon C} \simeq 0.57(5)$

Consistent!

Results of Numerical Bootstrap: $\sigma \times \sigma$ OPE (cont.)

Can take an irrelevant scalar as the middle operator ϵ' without greatly affecting OPE convergence

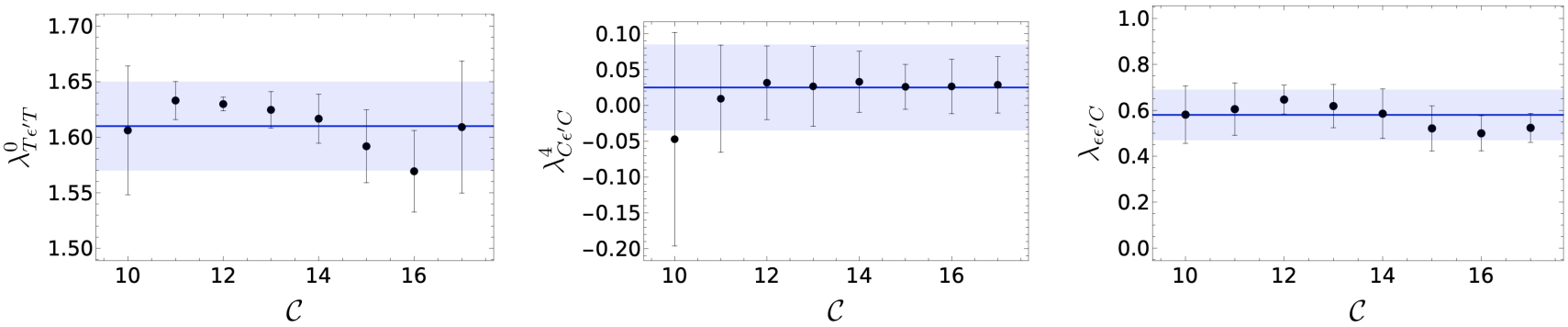

Figure: OPE coefficients computed from $\langle \sigma\sigma\epsilon'\sigma\sigma \rangle$ (without spin-6 contributions) by averaging over the minima of the cost function for the 20 sets of $\mathcal{C}$ constraints with the largest $\mathcal{I}$. Values determined by averaging the results with $11 \leqslant \mathcal{C} \leqslant 16$.

Results of Numerical Bootstrap: $\sigma \times \sigma$ OPE (cont.)

	est. values
$\lambda^0_{T\epsilon' T}$	1.61(4)
$\lambda^0_{T\epsilon' C}$	-1.2(3)
$\lambda^4_{C\epsilon' C}$	0.02(6)
$\lambda^3_{C\epsilon' C}$	2(2)
$\lambda^2_{C\epsilon' C}$	3(5)
$\lambda^1_{C\epsilon' C}$	-4(10)
$\lambda^0_{C\epsilon' C}$	3(8)
$\lambda_{\epsilon\epsilon' C}$	0.58(11)
$\lambda_{\epsilon'\epsilon' C}$	2.8(7)

Table: Numerical data for the unknown OPE coefficients in the truncated $\langle\sigma\sigma\epsilon'\sigma\sigma\rangle$ correlator, obtained from the 20 sets of constraints with the largest $\mathcal{I}$ for $11 \leqslant \mathcal{C} \leqslant 16$.

$\lambda^0_{T\epsilon T}$ and $\lambda^0_{T\epsilon' T}$: Bootstrap & Conformal Collider Bounds

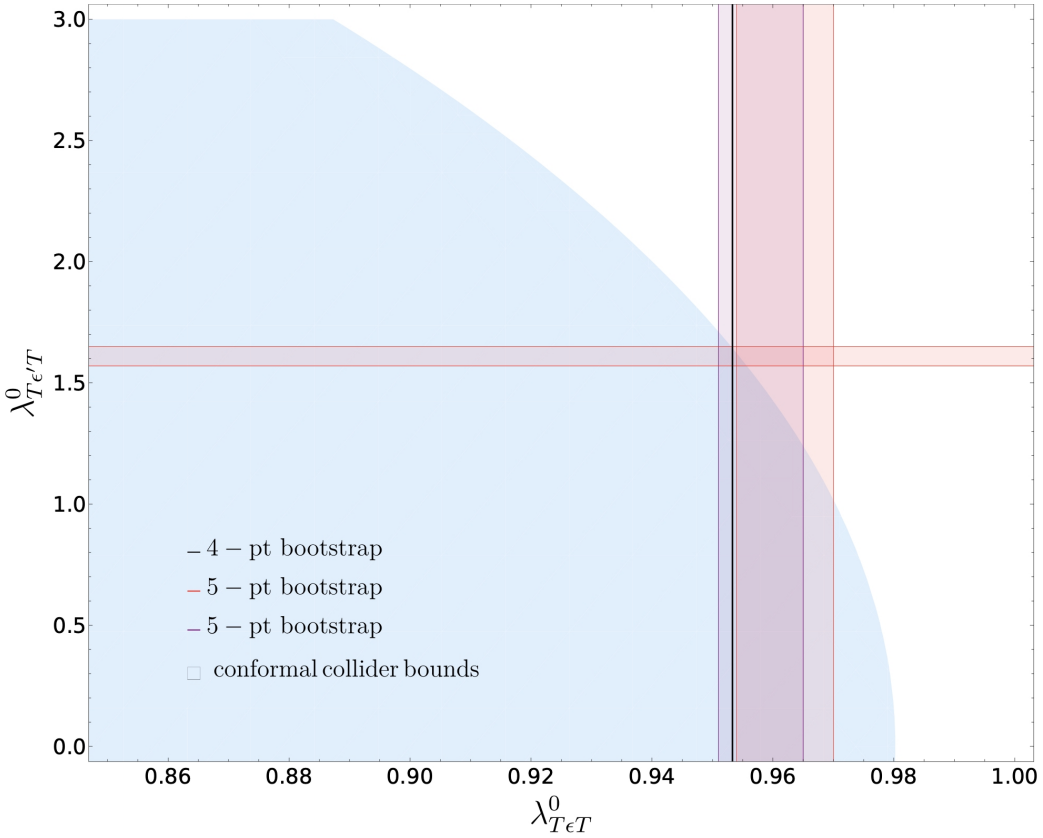

Figure: Conformal collider bounds on $\lambda^0_{T\epsilon T}$ and $\lambda^0_{T\epsilon' T}$ (blue region) Cordova et al. (2017) in addition to the value of $\lambda^0_{T\epsilon T}$ computed from the four-point bootstrap Chang et al. (2024) (black line).

Results of Numerical Bootstrap: $\sigma \times \epsilon$ OPE

Consider $\sigma \times \epsilon$ OPE and use truncation method to study

- $\langle \sigma\epsilon\epsilon\epsilon\sigma \rangle$, $\langle \sigma\epsilon\epsilon'\epsilon\sigma \rangle$, $\langle \sigma\sigma\sigma\sigma\epsilon \rangle$
- Determine OPE coefficients involving $\sigma, \epsilon, \epsilon'$, and $\Sigma_{\mu_1\mu_2\ldots\mu_\ell}$

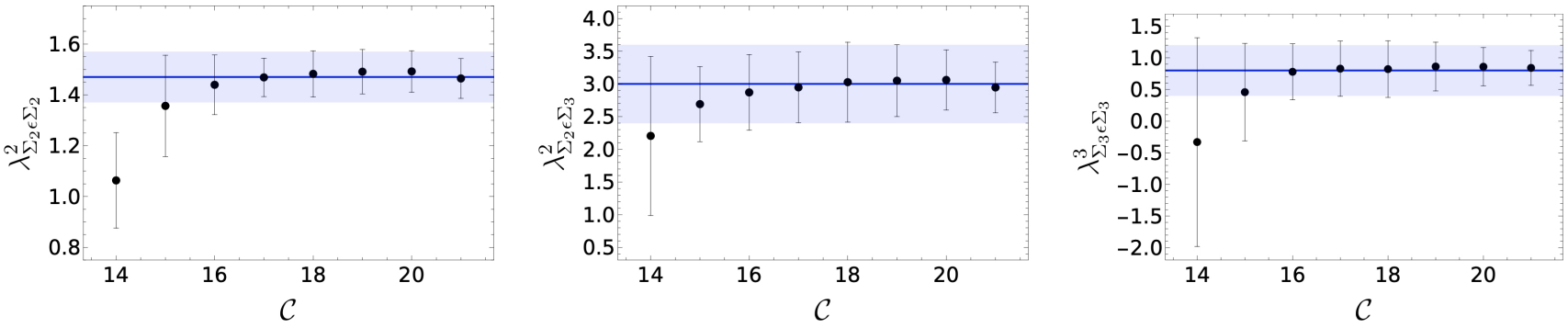

Figure: OPE coefficients computed from $\langle \sigma\epsilon\epsilon\epsilon\sigma \rangle$ by averaging over the minima of the cost function for the 20 sets of $\mathcal{C}$ constraints with the largest $\mathcal{I}$. Values determined by averaging the results with $16 \leqslant \mathcal{C} \leqslant 21$.

Results of Numerical Bootstrap: $\sigma \times \epsilon$ OPE (cont.)

	est. values
$\lambda^2_{\Sigma_2\epsilon\Sigma_2}$	1.47(10)
$\lambda^1_{\Sigma_2\epsilon\Sigma_2}$	-0.2(8)
$\lambda^0_{\Sigma_2\epsilon\Sigma_2}$	1.5(8)
$\lambda^3_{\Sigma_3\epsilon\Sigma_3}$	0.8(4)
$\lambda^2_{\Sigma_3\epsilon\Sigma_3}$	-7(3)
$\lambda^1_{\Sigma_3\epsilon\Sigma_3}$	7(3)
$\lambda^0_{\Sigma_3\epsilon\Sigma_3}$	-5(2)

	est. values
$\lambda^2_{\Sigma_2\epsilon\Sigma_3}$	3.0(6)
$\lambda^1_{\Sigma_2\epsilon\Sigma_3}$	3(2)
$\lambda^0_{\Sigma_2\epsilon\Sigma_3}$	-3(2)
$\lambda_{\sigma'\epsilon\Sigma_2}$	-1(2)
$\lambda_{\sigma'\epsilon\Sigma_3}$	-16(3)
$\lambda_{\sigma'\epsilon\sigma'}$	26(6)

Table: Numerical data for the unknown OPE coefficients in the truncated $\langle\sigma\epsilon\epsilon\epsilon\sigma\rangle$ correlator, obtained using the 20 sets of constraints with the largest $\mathcal{I}$ for $16 \leqslant \mathcal{C} \leqslant 21$.

Comments

- Large error bars for OPE coefficients involving σ', likely due to large twist
- Able to extract most accurate results for states on leading, lowest-twist Regge trajectory
- e.g. $\lambda_{\sigma'\epsilon\sigma'}$ comes with large standard deviation $\rightarrow$ sensitivity to number and choice of constraints
- Expect that 5-point bootstrap estimate not accurate
- Fuzzy sphere prediction: $|\lambda_{\sigma'\epsilon\sigma'}| \simeq 2.98(13)$ Hu, He, and Zhu (2023)

Results of Numerical Bootstrap: $\sigma \times \epsilon$ OPE (cont.)

Can take an irrelevant scalar as the middle operator ϵ' without greatly affecting OPE convergence

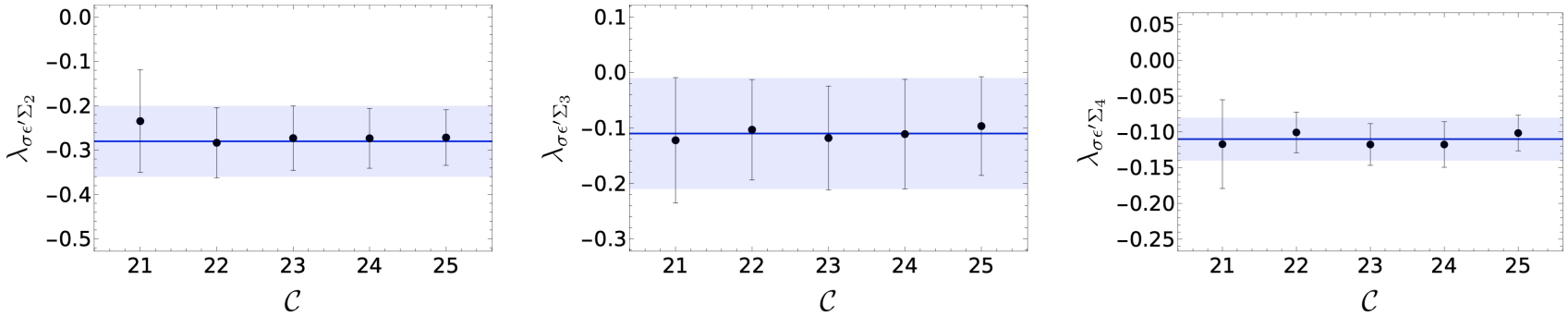

Figure: OPE coefficients computed from $\langle \sigma\epsilon\epsilon'\epsilon\sigma \rangle$ by averaging over the minima of the cost function for the 20 sets of $\mathcal{C}$ constraints with the largest $\mathcal{I}$. Values determined by averaging the results with $22 \leqslant \mathcal{C} \leqslant 25$.

Observe that relative errors larger than for $\langle \sigma\epsilon\epsilon\epsilon\sigma \rangle \to \Delta_{\epsilon'}$ is large

Results of Numerical Bootstrap: $\sigma \times \epsilon$ OPE (cont.)

	est. values
$\lambda_{\sigma\epsilon'\Sigma_2}$	-0.28(8)
$\lambda_{\sigma\epsilon'\Sigma_3}$	-0.11(10)
$\lambda_{\sigma\epsilon'\Sigma_4}$	-0.11(3)
$\lambda_{\sigma\epsilon'\Sigma_5}$	-0.03(8)
$\lambda_{\sigma\epsilon'\Sigma_6}$	-0.06(3)
$\lambda_{\sigma\epsilon'\Sigma_7}$	0.01(5)
$\lambda_{\sigma\epsilon'\sigma'}$	0.4(4)
$\lambda^2_{\Sigma_2\epsilon'\Sigma_2}$	0.0(5)
$\lambda^1_{\Sigma_2\epsilon'\Sigma_2}$	-7(2)
$\lambda^0_{\Sigma_2\epsilon'\Sigma_2}$	1(5)

	est. values
$\lambda^3_{\Sigma_3\epsilon'\Sigma_3}$	-0.7(7)
$\lambda^2_{\Sigma_3\epsilon'\Sigma_3}$	-7(7)
$\lambda^1_{\Sigma_3\epsilon'\Sigma_3}$	9(10)
$\lambda^0_{\Sigma_3\epsilon'\Sigma_3}$	-10(10)
$\lambda^2_{\Sigma_2\epsilon'\Sigma_3}$	0.7(7)
$\lambda^1_{\Sigma_2\epsilon'\Sigma_3}$	-5(6)
$\lambda^0_{\Sigma_2\epsilon'\Sigma_3}$	3(7)
$\lambda_{\sigma'\epsilon'\Sigma_2}$	9(3)
$\lambda_{\sigma'\epsilon'\Sigma_3}$	3(8)
$\lambda_{\sigma'\epsilon'\sigma'}$	12(11)

Table: Numerical data for the unknown OPE coefficients in the truncated $\langle\sigma\epsilon\epsilon'\epsilon\sigma\rangle$ correlator, obtained with the 20 sets of constraints with the largest $\mathcal{I}$ for $22 \leqslant \mathcal{C} \leqslant 25$.

- Can compare our $\lambda_{\sigma\epsilon'\Sigma_2} \simeq -0.28(8)$ to the fuzzy sphere result, $\lambda_{\sigma\epsilon'\Sigma_2} \simeq -0.365(2)$ Hu, He, and Zhu (2023)
- Falls within the error bar of our result

OPE Coefficients from the Fuzzy Sphere

Can accurately determine OPE coefficients in critical 3d Ising model by regularizing it on the fuzzy sphere Hu, He, and Zhu (2023)

We

- Compute some unknown OPE coefficients using fuzzy sphere method
- Compare fuzzy sphere predictions to 5-point bootstrap determinations

Observe agreement for OPE coefficients with relatively small error bars!

OPE Coefficients from the Fuzzy Sphere (cont.)

Hu, He, and Zhu (2023), Zhou (2025)

Example: $f_{\Sigma_2\epsilon\Sigma_2}$ on the fuzzy sphere

- Can represent ϵ by $n^x(\Omega)$:

$$\frac{\langle\Sigma_2, m=0|\int d\Omega\, Y_{0,0}(\Omega)n^x(\Omega)|\Sigma_2, m=0\rangle - \langle 0|\int d\Omega\, Y_{0,0}(\Omega)n^x(\Omega)|0\rangle}{\langle\epsilon|\int d\Omega\, Y_{0,0}(\Omega)n^x(\Omega)|0\rangle} = f_{\Sigma_2\epsilon\Sigma_2} + \frac{c_1}{N^{\frac{\Delta_T-\Delta_\epsilon}{2}}} + \frac{c_2}{N} + \mathcal{O}\left(N^{-\frac{\Delta_{\epsilon'}-\Delta_\epsilon}{2}}\right) \tag{30}$$

- In standard box basis:

$$f_{\Sigma_2\epsilon\Sigma_2} = \lambda^2_{\Sigma_2\epsilon\Sigma_2} - \frac{1}{3}\lambda^1_{\Sigma_2\epsilon\Sigma_2} + \frac{2}{15}\lambda^0_{\Sigma_2\epsilon\Sigma_2} \tag{31}$$

- Result from 5-point bootstrap: $f_{\Sigma_2\epsilon\Sigma_2} \simeq 1.7(2)$
- Agrees with fuzzy sphere result! (also note: $f_{\Sigma_2\epsilon\Sigma_2} \simeq 1.46$ in Herviou, Läuchli, Rychkov, and Wilhelm (2025))

OPE Coefficients from the Fuzzy Sphere (cont.)

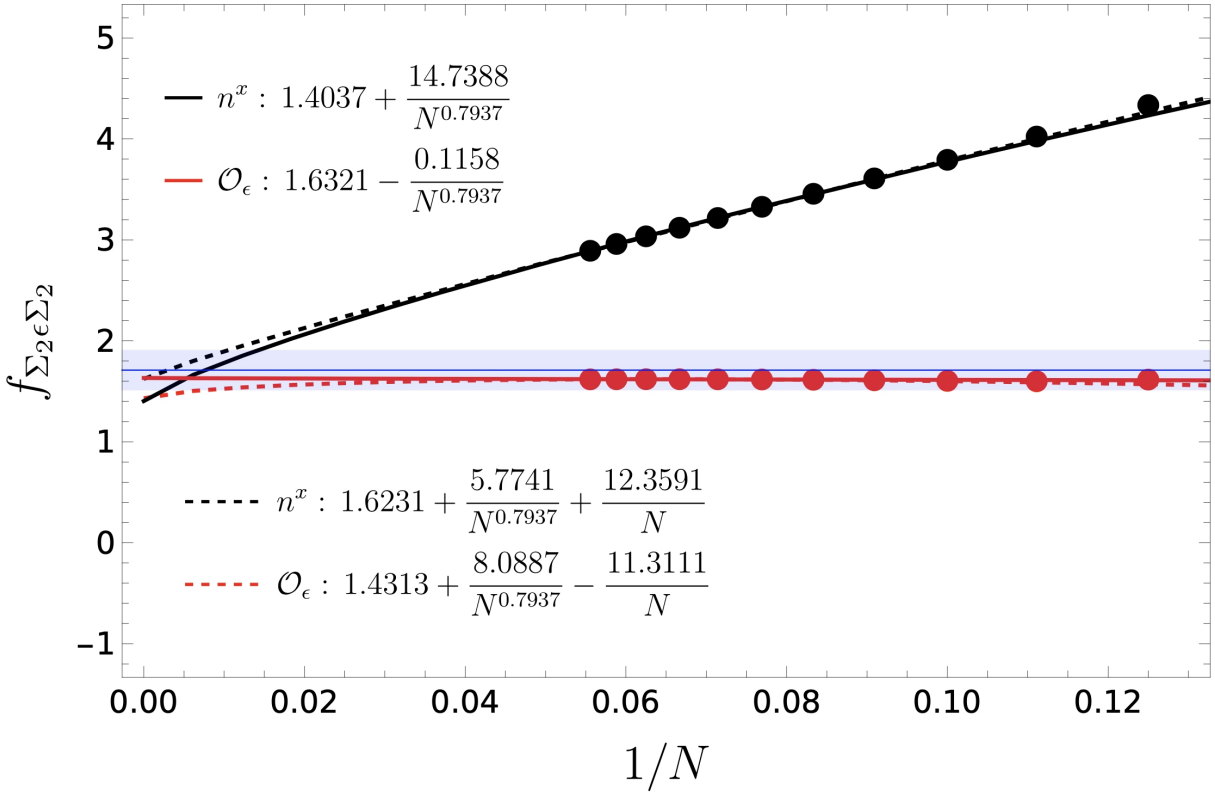

Figure: Fuzzy sphere results for $f_{\Sigma_2 \epsilon \Sigma_2}$. The black and red dots and fits represent different ways in which the ϵ operator can be represented on the fuzzy sphere. Fitting performed using the 6 points with the largest N.

Preview: Six-Point Bootstrap in the Snowflake Channel

Generalize approach of Poland, VP, Tadić (2023) to case of six-point scalar correlators in snowflake channel

$$\langle \phi_1(x_1)\phi_2(x_2)\phi_3(x_3)\phi_4(x_4)\phi_5(x_5)\phi_6(x_6)\rangle = \sum_{(\mathcal{O}_{\Delta,\ell},\mathcal{O}'_{\Delta',\ell'},\mathcal{O}''_{\Delta'',\ell''})} \sum_{n_{12}=0}^{\min(\ell,\ell')} \sum_{n_{13}=0}^{\min(\ell,\ell'')} \sum_{n_{23}=0}^{\min(\ell',\ell'')} \lambda_{\phi_1\phi_2\mathcal{O}_{\Delta,\ell}} \lambda_{\phi_3\phi_4\mathcal{O}'_{\Delta',\ell'}} \lambda_{\phi_5\phi_6\mathcal{O}''_{\Delta'',\ell''}} \times \lambda^{(n_{12}n_{13}n_{23})}_{\mathcal{O}_{\Delta,\ell}\mathcal{O}'_{\Delta',\ell'}\mathcal{O}''_{\Delta'',\ell''}} P(x_i) G^{(n_{12},n_{13},n_{23})}_{(\Delta,\ell,\Delta',\ell',\Delta'',\ell'')}(u_1, v_1, u_2, v_2, u_3, v_3, U_1, U_2, U_3) \tag{32}$$

Define generalized radial coordinates $(R, r, r', \eta_1, \eta_2, \eta_3, \bar{w}_1, \bar{w}_2, \bar{w}_3)$ and consider monomial ansatz

Preview: Six-Point Bootstrap in the Snowflake Channel (cont.)

Ansatz:

$$G^{(n_{12},n_{13},n_{23})}_{(\Delta,\ell,\Delta',\ell',\Delta'',\ell'')}(R,r,r',\eta_1,\eta_2,\eta_3,\bar{w}_1,\bar{w}_2,\bar{w}_3) = \sum_{n_1=0}^{\infty}\sum_{n_2}\sum_{n_3}\sum_{j,j',j''}\sum_{m=0}^{\min(j,j')}\sum_{m'=0}^{\min(j,j'')}\sum_{m''=0}^{\min(j',j'')}$$
$$B_{\left(\frac{n_1+n_2}{3},\frac{n_1-n_2+n_3}{3},\frac{n_1-n_3}{3};j,j',j'';m,m',m''\right)} R^{\Delta+\Delta'+\Delta''+n_1} r^{2\Delta-\Delta'-\Delta''+n_2} r'^{\Delta+\Delta'-2\Delta''+n_3} \times$$
$$\eta_1^{j-m-m'}\eta_2^{j'-m-m''}\eta_3^{j''-m'-m''}\bar{w}_1^{m}\bar{w}_2^{m''}\bar{w}_3^{m'}, \tag{33}$$

where e.g.

$$n_2 \in [-n_1, -n_1+3, \ldots, 2n_1-3, 2n_1],$$
$$j \in \left[\ell + \frac{n_1+n_2}{3}, \ell + \frac{n_1+n_2}{3} - 2, \ldots, \left(\ell + \frac{n_1+n_2}{3}\right) \bmod 2\right]. \tag{34}$$

- Determine B-coefficients analogously
- Use Padé approximant to accelerate convergence

Preview: Six-Point Bootstrap in the Snowflake Channel (cont.)

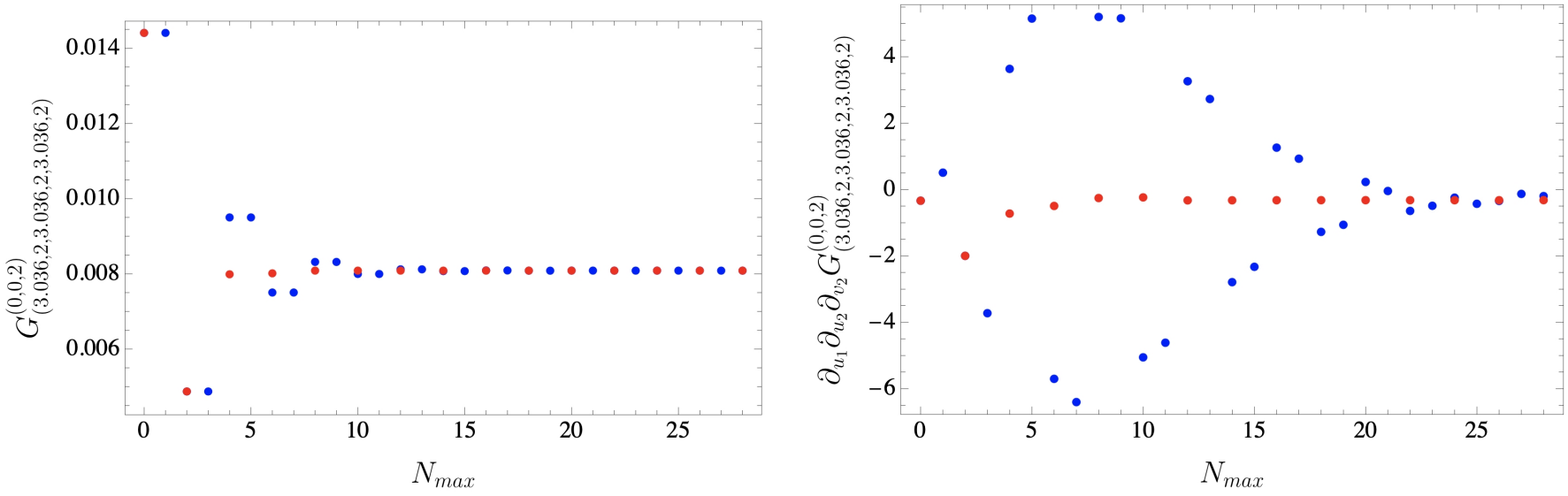

Figure: The six-point snowflake channel conformal block and one of its derivatives with exchanged operators of spins 2, 2, 2 with the following choice of parameters: $\ell = \ell' = \ell'' = 2$, $n_{12} = 0$, $n_{13} = 0$, $n_{23} = 2$, $\Delta = \Delta' = \Delta'' = 3.0363$ evaluated at $R = 3 - 2\sqrt{2}$, $r = 1$, $r' = 1$, $\eta_1 = 1$, $\eta_2 = 1$, $\eta_3 = 1$, $\bar{w}_1 = 0$, $\bar{w}_2 = 0$, $\bar{w}_3 = 0$.

Preview: Six-Point Bootstrap in the Snowflake Channel (cont.)

- Study $\langle\sigma\sigma\sigma\sigma\sigma\sigma\rangle$ in 3d critical Ising using analogous approach
- Truncate the operator spectrum, e.g. up to spin 2
- Approximate truncated portion by MFT correlator $\langle\sigma\sigma\sigma\sigma\sigma\sigma\rangle_{\mathrm{MFT}}$, e.g. $\mathcal{S}_{\mathrm{Ising}} = \{\mathbb{1}, \epsilon, \epsilon', T_{\mu\nu}\} \leftrightarrow \mathcal{S}_{\mathrm{MFT}} = \{\mathbb{1}, [\sigma,\sigma]_{0,0}, [\sigma,\sigma]_{1,0}, [\sigma,\sigma]_{0,2}\}$
- Implement same bootstrap procedure as in five-point case

Conclusions

- Presented an algorithm for the numerical evaluation of five-point conformal blocks similar to approach of Costa et al. (2016) for four-point blocks
- Evaluated five-point blocks (and derivatives) using a Padé approximant
- Studied 5-point correlators of σ, ϵ, and ϵ' in the 3d critical Ising model via truncation method of Gliozzi (2013), Gliozzi and Rago (2014)

Conclusions (cont.)

- Approximated truncated part of a correlator with contributions from a disconnected five-point correlator
- Computed a number of unknown OPE coefficients
- Compared results to fuzzy sphere counterparts $\rightarrow$ good agreement for well-determined OPE coefficients
- Presented a preview of this approach in 6-point snowflake channel

Conclusions (cont.)

Future Work

- Apply truncation+approximation+4-point method to other theories, e.g. models with global $O(2)$ and $O(3)$ Chester et al. (2020, 2021), Liu et al. (2020)
- Study five-point correlators in non-unitary CFTs, such as Lee-Yang models Gliozzi and Rago (2014), Arguello Cruz et al. (2025), Miro & Delouche (2025)
- Explore how machine learning techniques could further improve these methods Kántor et al. (2022)

THANK YOU!

Backup Slides

The Mean-Field Theory (MFT) Approximation: A Four-Point Example

Consider $\langle\sigma\sigma\sigma\sigma\rangle$ in 3d critical Ising Model

- Expand $\langle\sigma\sigma\sigma\sigma\rangle$ in terms of conformal blocks $g_{\Delta,l}$ in the (12)(34) OPE channel

$$\langle\sigma(x_1)\sigma(x_2)\sigma(x_3)\sigma(x_4)\rangle = \frac{1}{x_{12}^{2\Delta_\sigma} x_{34}^{2\Delta_\sigma}} \sum_{\mathcal{O}_{\Delta,l}} \left(\lambda_{\sigma\sigma\mathcal{O}_{\Delta,l}}\right)^2 g_{\Delta,l}(u,v) \tag{35}$$

- Cross-ratios: $u = \frac{x_{12}^2 x_{34}^2}{x_{13}^2 x_{24}^2}$ and $v = \frac{x_{14}^2 x_{23}^2}{x_{13}^2 x_{24}^2}$
- Can also write the expansion in the (14)(23) channel and demand that the two expansions agree

The Mean-Field Theory (MFT) Approximation: A Four-Point Example (cont.)

As in Gliozzi (2013), Gliozzi and Rago (2014), we

- Truncate the $\sigma \times \sigma$ operator product expansion (OPE) to include only operators with conformal dimension below a cutoff $\Delta_{\text{cutoff}} \approx 5.022$
- Only include operators in $\mathcal{X} = \{\epsilon, \epsilon', T_{\mu\nu}, C_{\mu\nu\rho\sigma}\}$
- ϵ is the leading $\mathbb{Z}_2$-even scalar, T is the spin-2 stress tensor, and C is the leading spin-4, $\mathbb{Z}_2$-even operator
- Fix conformal dimensions of all exchanged operators Simmons-Duffin (2016)

$$\Delta_\epsilon = 1.412625\,, \quad \Delta_{\epsilon'} = 3.82968\,, \quad \Delta_C = 5.022665 \tag{36}$$

The Mean-Field Theory (MFT) Approximation: A Four-Point Example (cont.)

But treat Δ_σ and all OPE coefficients as unknown

$$\mathcal{P}[\mathcal{O}_{\Delta,l}] = \left(\lambda_{\sigma\sigma\mathcal{O}_{\Delta,l}}\right)^2 \tag{37}$$

- Approximate all truncated contributions with the corresponding MFT contributions
- Double-twist operators $[\sigma\sigma]_{n,l}$ of dimension $2\Delta_\sigma^{MFT} + 2n + l$ and spin l in $\mathcal{X}_{MFT} = \{[\sigma,\sigma]_{0,0}, [\sigma,\sigma]_{1,0}, [\sigma,\sigma]_{0,2}, [\sigma,\sigma]_{0,4}\}$

The Mean-Field Theory (MFT) Approximation: A Four-Point Example (cont.)

Results:

	no MFT	with MFT	Simmons – Duffin (2016)
Δ_σ	0.514(5)	0.5182(4)	0.5181489(10)
$\mathcal{P}[\epsilon]$	1.15(4)	1.106(5)	1.106396(9)
$\mathcal{P}[\epsilon']$	-0.010(8)	0.003(2)	0.002810(6)
$\mathcal{P}[T_{\mu\nu}]$	0.33(5)	0.422(2)	0.425463(1)
$\mathcal{P}[C_{\mu\nu\rho\sigma}]$	0.115(9)	0.0768(5)	0.0763(1)

Table: Numerical data for Δ_σ and the unknown OPE coefficients in $\langle\sigma\sigma\sigma\sigma\rangle$ without or with the MFT approximation, compared with the best results for these parameters from Simmons-Duffin (2016)

Compute conformal dimensions of operators below the cutoff more accurately than in Gliozzi (2013), Gliozzi and Rago (2014), as demonstrated in Li (2023)

Convergence of Higher-Point Conformal Blocks

Consider

$$\langle \phi(x)\phi(y)\prod \psi_i(z_i)\rangle = \sum_{\mathcal{O}} \lambda_{\phi\phi\mathcal{O}} C_{\mathcal{O}}(x-y,\partial_y)\langle \mathcal{O}(y)\prod \psi_i(z_i)\rangle \tag{38}$$

Convergence: Always possible to draw a sphere that separates $\phi(x)$ and $\phi(y)$ from the $\psi_i(z_i)$!

Example: 6-point case

- Conformal frame s.t. x_2, x_4, and x_5 are collinear, while x_1, x_3, and x_6 lie on 3 planes that intersect at this line
- Impossible to draw a sphere if any two planes collapse onto each other!
- $U_1 \propto x_{13}^2, U_2 \propto x_{36}^2, U_3 \propto x_{16}^2$
- Occurs if some $U_i = 0 : U_1 = 0, U_2 = 0, U_3 = 0$

Convergence of Higher-Point Conformal Blocks (cont.)

- Cast conditions in terms of radial coordinates $\{R, r, r', \eta_1, \eta_2, \eta_3, \bar{w}_1, \bar{w}_2, \bar{w}_3\}$
- Solve each condition for R: R_i^j, where $i = 1, 2, 3$ and $j = 1, \ldots, 8$
- Fix $\{r, r', \eta_1, \eta_2, \eta_3, \bar{w}_1, \bar{w}_2, \bar{w}_3\}$
- Select minimum solution

$$R^* = \min[R_1^i, R_2^j, R_3^k], \qquad R_i^j > 0, \quad R_i^j \in \mathbb{R} \tag{39}$$

$\Rightarrow$ R^* is the radius of convergence of the conformal block!

If block converges, its Padé approximant converges to the same value